ACS APPLIED BIO MATERIALS

www.acsabm.org Article

Fabrication of a pH/Redox-Triggered Mesoporous Silica-Based Nanoparticle with Microfluidics for Anticancer Drugs Doxorubicin and Paclitaxel Codelivery

Jiaqi Yan,[⊥] Xiaoyu Xu,[⊥] Junnian Zhou, Chang Liu, Lirong Zhang, Dongqing Wang, Fan Yang,* and Hongbo Zhang*

Cite This: *ACS Appl. Bio Mater.* 2020, 3, 1216–1225 Read Online

ACCESS | Metrics & More | Article Recommendations | Supporting Information

ABSTRACT: A pH/redox-triggered mesoporous silica nanoparticle (MSN)-based nanoplatform has been fabricated for doxorubicin/paclitaxel (DOX/PTX) codelivery. In this drug-delivery system (DDS), PTX is covalently attached to the surface of DOX loaded MSN via a linker with disulfide bond. By directly attaching PTX to MSN, we can significantly enhance the PTX's loading degree and achieve the optimum drug loading ratio to DOX, therefore, to generate the best synergistical effect. More importantly, PTX and the linker act as a redox-sensitive "gate" to precisely control the release profile of DOX and PTX. Subsequently, polystyrenesulfonate (PSS) is electrostatically coated to DOX loaded MSN-PTX in microfluidics to achieve acidic pH responsive, because the free amino group on MSN surface has a protonation state at acidic pH, and the electrostatic interaction will be destroyed at pH 5. In addition, PSS can also neutralize the surface zeta potential, thus reduce the nonspecific endocytosis of healthy cells. By evaluating cell viability in cancer cell BT549 and healthy breast cell MCF-10A, we observed that the nanoparticles can selectively release DOX and PTX and eliminate cancer cells, while they will have negligible effect on the healthy breast cells, due to the acidic and redox microenvironment in cancer cells. Overall, we have developed a nanoplatform for precise DOX/PTX combination therapy with high selectivity between cancer cells and healthy cells.

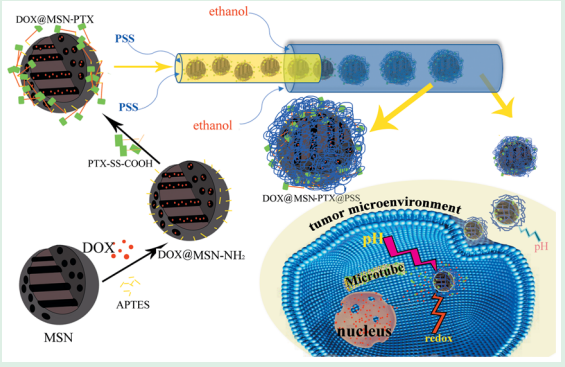

KEYWORDS: *mesoporous silica nanoparticles, doxorubicin, paclitaxel, pH/redox-triggered release, microfluidic technology, combination therapy*

1. INTRODUCTION

During the past decades, the incidence and mortality of cancer is continually increasing, posing challenges for the current medication.[1,2] Nowadays, the main clinical cancer treatments include surgery, radiotherapy, and chemotherapy.[3,4] Among them, chemotherapy is the most accessible therapeutic option for tumors. Most chemotherapy drugs lack tumor site targeting;[5−9] and the use of a single chemotherapeutic agent often causes adverse drug effects and drug resistance.[10−12] Hence, preparing drug delivery systems (DDS) to improve drug selectivity and enable the combination therapy is of great importance.

Nanoparticles (NPs) based DDSs hold lots of advantages, including targeting the tumor sites, prolonging circulation time, and improving bioavailability.[5−8] Among the nanocarriers reported, MSN is one of the most extensively studied nanoparticles for smart drug delivery.[13−17] The MSN-based nanodelivery system presents lots of outstanding properties, such as good biocompatibility, easy chemical modification, and high encapsulation capacity.[18−20] In the process of the high selectivity of drug-loaded NPs, besides utilizing the enhanced permeability and retention effect (EPR effect) that nanoparticles will passively aggregate at the tumor site, it is also possible to selectively kill tumor cells by designing the nanoparticles with tumor microenvironment triggered drug release.[21−24] Since there are multiple stimuli at the tumor site, the carrier with multiple stimuli response can more precisely deliver the drugs as compared to a single stimuli.[25,26] The combination of Doxorubicin (DOX) and Paclitaxel (PTX) is an effective and active treatment for many solid tumors. DOX is a family of anthracycline antibiotics that binds to DNA and inhibits nucleic acid synthesis. PTX can promote microtubule assembly and lead to apoptosis. The combination of DOX and PTX has been used as important conventional chemo-

Received: December 3, 2019
Accepted: January 19, 2020
Published: January 19, 2020

https://dx.doi.org/10.1021/acsabm.9b01111
ACS Appl. Bio Mater. 2020, 3, 1216–1225

Scheme 1. Schematic Illustration of the Synthesis of DOX@MSN-PTX; and the Microfluidic Fabrication of DOX@MSN-PTX@PSS[a]

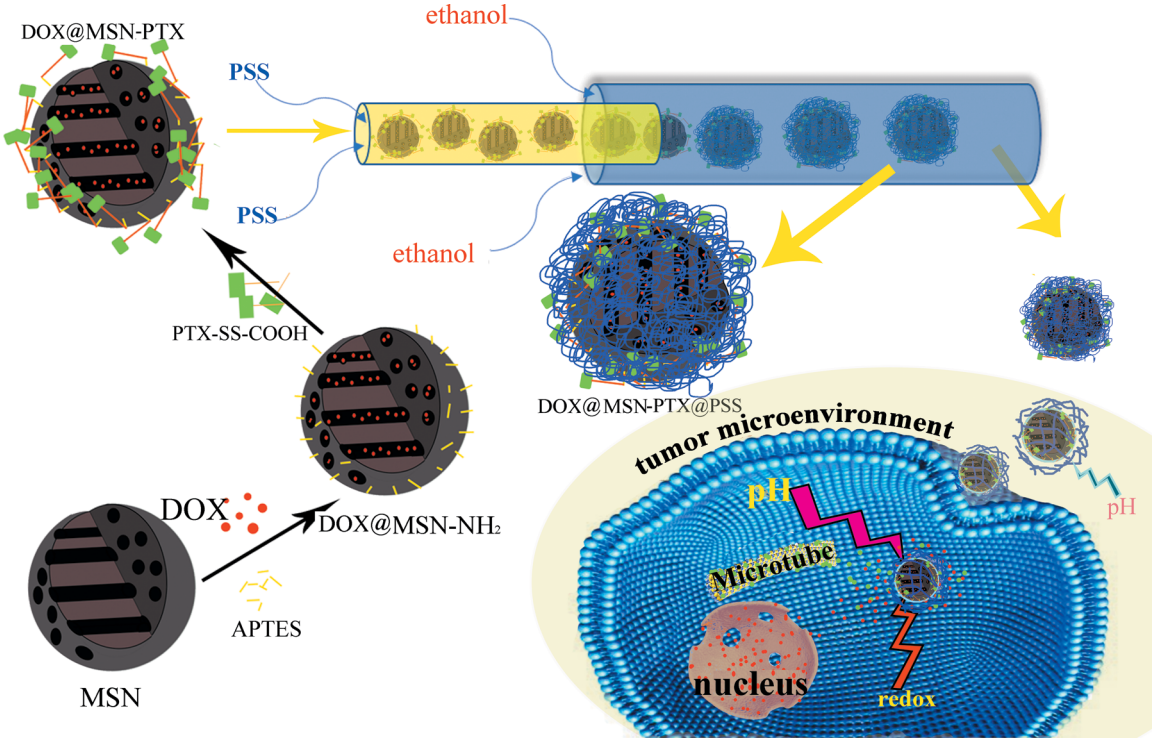

[a]The PSS layer swells under acidic tumor microenvironment; thus the DOX@MSN-PTX@PSS becomes positively charged and can be internalized by tumor cells via endocytosis. Subsequently, the pH/redox condition in tumor cells can induce the DOX and PTX release inside the tumor cells.

therapeutic agents because of their different action mechanisms; however, it has been reported that the ratio of DOX to PTX plays a critical role in the synergistical effect but due to the distinct water solubility, the DOX/PTX combination has rarely achieved optimum synergistic.[27,28] Moreover, both drugs have adverse drug effects if systemically dosed.

In this work, As revealed in Scheme 1, DOX is loaded into MSN, but PTX is conjugated with MSN through a redox-sensitive linker, which can enhance and control the loading degree, solubility, stability of the hydrophobic drug PTX. The loading ratio of DOX and PTX is precisely controlled to optimize the synergistic effect by accurately controlling the content of covalently linked PTX. Moreover, the redox sensitive linker can also control the PTX and DOX release simultaneously.

Polystyrenesulfonate (PSS) is an electronegative polymer with high biocompatibility[29] which can produce electrostatic attraction with free amino groups on the surface of MSN. To prevent the PTXs direct expose to physiological environment and further increase the tumor specificity of nanoparticles, PSS is coated on top of DOX loaded MSN-PTX via microfluidics, which has been widely used for nanoparticle fabrication and nanocomponents related drug loading and delivery.[30−32] Basically, microfluidics technology can be used to process very small quantities of samples, and the size, shape and functional surface of the fabricated nanoparticles can also be tuned. These advantages can facilitate drug delivery and control the release profiles. In addition, because the parameters can be precisely controlled, microfluidics can also scale up production.[33−35] The coating of PSS with microfluidics can completely seal the pores on MSN, and control the drug release under the acidic condition, as found in tumor microenvironments.[36] Moreover, PSS can also inhibit the unspecific cell uptake by adjusting the zeta potential to neutral.[37] At last, the effects and selectivity of this nanoparticle between cancer cells and healthy cells are evaluated with breast cancer cell BT549 and healthy breast cell MCF-10.

2. EXPERIMENTAL SECTION

2.1. Materials. Doxorubicin (DOX) and Paclitaxel (PTX) were purchased from Arisun ChemPharm Co., Ltd. (China). Cetyltrimethylammonium chloride (CTAC); tetraethyl orthosilicate (TEOS); triethanolamine (TEA); 1-octadecene; ammonium nitrate (NH4NO3); 3-aminopropyltriethoxysilane (APTES) and ethanol solution were purchased from Sigma-Aldrich (Finland). 4-dimethylaminopyridine (DMAP), 3,3′-dithiodipropionic acid (DTDP) and *N*-(3-(dimethylamino)propyl)-*N*-ethylcarbodiimide hydrochloride (EDC·HCl) were purchased from Alfa Aesar (Finland). Dichloromethane (DCM), DL-dithiothreitol (DTT), triethylamine, acetyl chloride, were also purchased from Sigma-Aldrich (Finland).

2.2. Preparation and the Characterization of PTX-S-S-COOH (Paclitaxel Conjugate with DTDP). The synthesis and characterization of dithiodipropionic anhydride (DTDPA) and PTX-S-S-COOH are described in the previous literature.[5,38−40] The details are provided in the Supporting Information (SI).

2.3. Synthesis MSN and MSN-NH_2. MSN was synthesized as previously reported.[41] MSN-NH_2 was made by refluxing 200 mg MSN and 200 μL APTES in ethanol overnight. Then centrifuged at 16 000 rpm to obtain the crude product, which was washed with ethanol three times to obtain the Amine-functionalized MSN. The details are provided in the SI.

2.4. Synthesis of MSN-PTX and Different Molar Ratio Drug Loading. *2.4.1. Synthesis Different (DOX: PTX) Drug Molar Ratio of DOX@MSN-PTX (DOX: PTX = 1:10; 1:5; 1:0.588).* Basically, we first control the loading content of DOX by loading time, and then we add the same amount of PTX-SS-COOH to control the amount of PTX unchanged. The details are provided in the SI.

https://dx.doi.org/10.1021/acsabm.9b01111
ACS Appl. Bio Mater. 2020, 3, 1216−1225

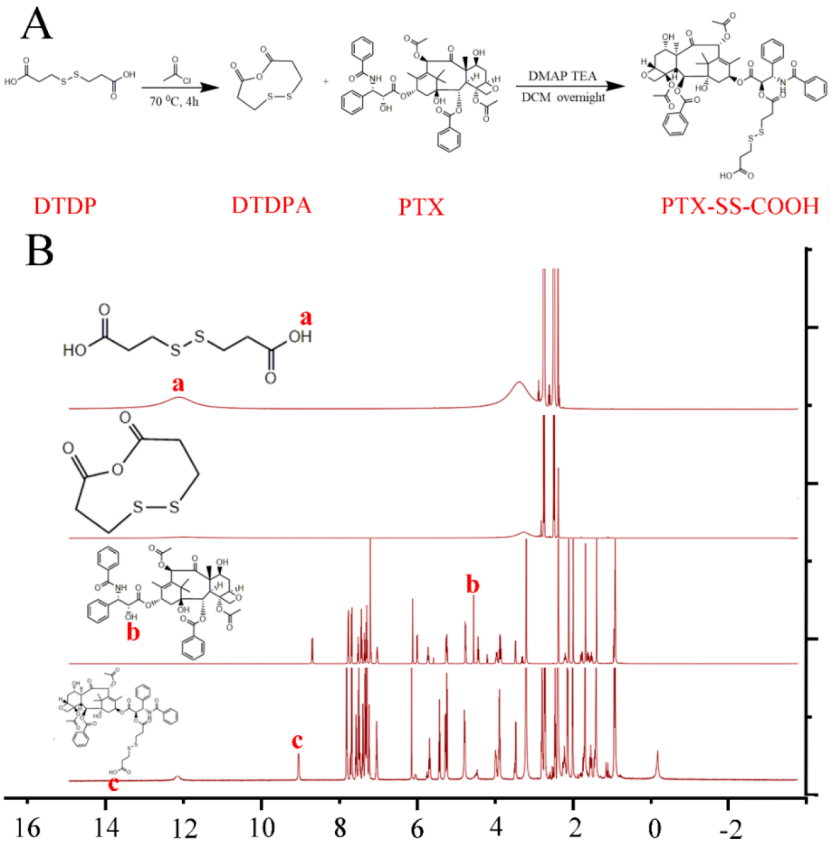

Figure 1. (A) the synthesis route of PTX-SS-COOH; (B) the ^{1}H NMR spectra of DTDP in DMSO-d_6, DTDPA in CDCl3, PTX in $CDCl_3$, PTX-SS-COOH in DMSO-d_6.

2.4.2. Characterization of Drug Loading and Encapsulation Efficiency. The DOX and PTX loading content (LC (%) = (loaded drug (DOX/PTX)/weight of nanoparticles ×100) and entrapment efficiency (EE (%) = (loaded drug (DOX/PTX)/added drug (DOX/PTX) weight ×100) were quantified by UV−vis spectroscopy at 490 nm and gradient analytical HPLC assay, respectively. HPLC assay was performed on an Agilent 1100 instrument, and 20 μL of solution was loaded onto Waters reverse phase column (250 × 4.6 mm). Acetonitrile (TFA 0.1%):water (TFA 0.1%) (acetonitrile increases from 5 to 95% with 20 min) was eluted at 1 mL/min, and the PTX were detected at 254 nm by a UV detector (UV-975, Jasco). The loaded drug was calculated by using the whole amount of added drug minus all the amount of drug within supernatant which was collected after each centrifugation.

2.5. Preparation of DOX@MSN-PTX@PSS. We encapsulate DOX @ MSN-PTX in a PSS polymer by using a microfluidic device. Instrument parameters and preparation methods are as described in the previous article.[30,31,42,43] All the details are provided in the SI.

2.6. The in Vitro Release of DOX and PTX from the Nanoparticles. DOX@MSN-PTX@PSS were sonicated uniformly in 1.0 mL of PBS buffer solution (pH5 with DTT; pH5 without DTT; pH7 with DTT; pH7 without DTT) and then, put it into PBS buffer at 37 °C, continually shaking in the darkroom. At selected intervals, the buffer was centrifuged at 16 000 rpm, then the 0.9 mL supernatant was withdrawn and analyzed by fluorescence spectrum. Subsequently, 0.9 mL fresh medium was returned to the original solution and sonicated until nanoparticles dispersed well then put back into the shaker. The UV−vis spectral standard curve of doxorubicin is $Y_1 = 0.02083X_1 - 0.00399$ ($R = 0.9998$) Here Y_1 is UV absorption integral of DOX at 490 nm wavelengths; X_1 is the concentration of DOX(μg), and the standard curve detected by HPLC for paclitaxel is $Y_2 = 0.03311X_2 - 0.04503$ ($R = 0.9997$) Here Y_2 is UV absorption integral of PTX at 230 nm wavelengths; X_2 is the concentration of PTX(μg).

2.7. Characterization of the PTX-SS-COOH and Nanoparticles. The blank MSN, DOX@MSN-PTX, DOX@MSN-PTX@PSS was evaluated by using The ^{1}H NMR, MS, FTIR, Zetasizer Nano ZS and the transmission electron microscope (TEM). Methods and instrument parameter are described in the SI.

2.8. Biocompatibility and Particle Cell Interaction. Cell culture, maintenance, and cytotoxicity assays were studied in human breast cancer cell BT-549 and health cell MCF-10A. WST-1 cell viability assay and Multimode microplate reader were used for cytotoxicity assays. Doxorubicin localization and cellular uptake study are detected by confocal microscopy and flow cytometer. All the details are provided in the SI.

3. RESULTS AND DISCUSSION

3.1. Synthesize and Characterization of PTX-SS-COOH. In order to enhance the PTX loading capacity, tumor targeting specificity and achieve the optimum drug loading ratio to DOX, we conjugated PTX to MSN through a redox-sensitive liner. As shown in Figure 1A, PTX is first conjugated with the redox-sensitive linker to form the PTX-SS-COOH through a two-step reaction. DTDP is a commercially available redox-sensitive linker, while the directly esterification with PTX will result in byproduct formation because DTDP has two active carboxyl groups to react with PTX. Therefore, the DTDP is converted to DTDPA, then it is conjugated with PTX.

^{1}H NMR spectra of PTX-SS-COOH and its intermediate products are shown in Figure 1B. The peak of −COOH group of DTDP at 12.35 ppm (Figure 1B (a)) disappeared after refluxing in acetyl chloride at 70 °C and turning to the circle. Moreover, the DTDP powder melts to a clear and transparent solution after refluxing at 70 °C which suggests that the

https://dx.doi.org/10.1021/acsabm.9b01111
ACS Appl. Bio Mater. 2020, 3, 1216−1225

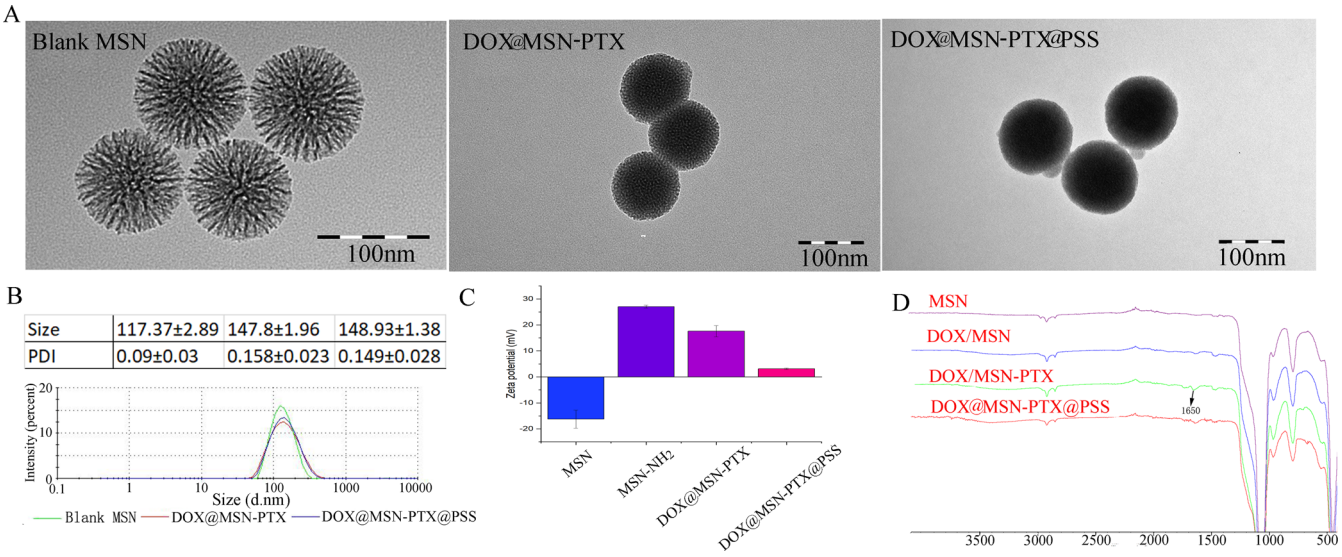

Figure 2. Characterization of DOX@MSN-PTX@PSS nanoparticles. (A) TEM images (B) Size and PDI results from DLS. (C) the zeta potential of MSN; DOX@MSN-NH_2; DOX@MSN-PTX; DOX@MSN-PTX@PSS (n = 3) and (D) FTIR spectra.

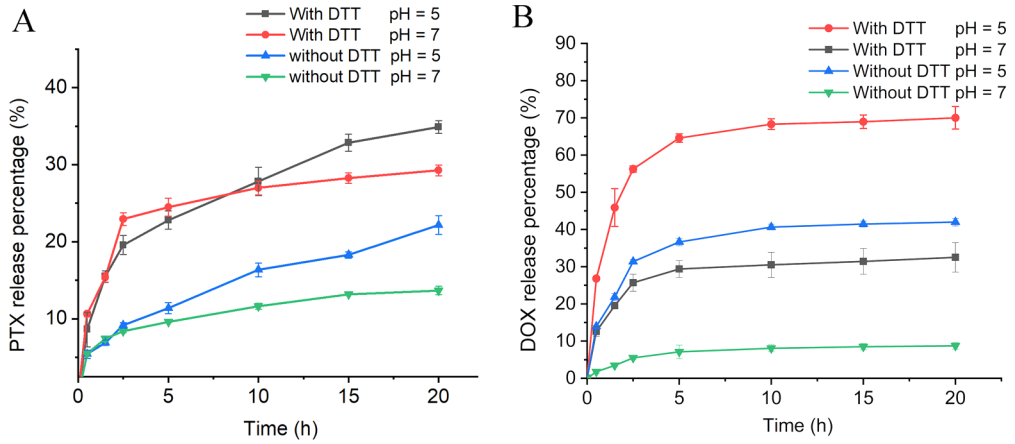

Figure 3. (A) The in vitro release of PTX from NPs; (B) The in vitro release of DOX from NPs. (molar ratio of DOX: PTX = 1:0.588).

melting point shifted from 153 to 155 to 70 °C, which also confirms the successful synthesis of DTDPA.[40]

For the conjugation between PTX and DTDPA, the 2′-OH proton peak of PTX at 4.7 ppm disappeared (Figure 1B (b)), which is the most active reactive site to react with DTDPA.[44] In addition, the −COOH group showed up again but shifted to 9.4 ppm (Figure 1B (c)), indicating the opening of the circle.[40] The MS^- spectra of PTX-SS-COOH shown in SI Figure S1 gives a sharp peak at mass of 1044.3134, which is almost identical to the calculated mass of 1044.3152, and the 2090.6350 peak equals to the PTX-SS-COOH dimer. Moreover, As shown in SI Figure S2, the HPLC characterization of PTX and PTX-SS-COOH showed single peak with a retention time of 13.296 and 4.998 min, respectively. The results of HPLC, MS, and NMR together confirm that the PTS-SS-COOH is successfully synthesized.

3.2. Synthesize and Characterization of MSN, DOX@MSN-PTX, DOX@MSN-PTX@PSS, Nanoparticles. MSN was prepared in an oil−water two-phase layered reaction system.[41] The oil phase is composed by a TEOS solvent with 1-octadecene, and the water phase is containing CTAC and TEA as a template and catalyst, respectively.

MSN was successfully synthesized with uniform porous sphere structure in TEM (Figure 2A). The DLS results showed that MSN was around 117.37 nm (Figure 2B) and zeta potential was around −19 mV (Figure 2C). The negative charge of MSN is due to the presence of −OH groups on the surface. Whereas, after modifying the MSN with APTES, the zeta potential dramatically increased to positive (around 28 mV) (Figure 2C). To conjugate with PTX, TEM results showed that the surface pores of DOX@MSN-PTX become unclear, and the particle size was around 100 nm (Figure 2A), while DLS showed that the DOX@MSN-PTX was about 150 nm (Figure 2B). Since TEM requires observing the sample in the dry state, whereas DLS allows the samples to be observed in a solvated state, where there will be particles associated with solvent molecules, the size detected in DLS is generally bigger than in TEM.[45] Moreover, after the esterification between PTX-SS-COOH and MSN, the zeta potential shows a small decline to 15 mV, but it is still positive (Figure 2C).It suggested that there was still an unsaturated $-NH_2$ group in existence. Furthermore, the FTIR spectra showed that after the esterification of PTX-SS-COOH with $-NH_2$, an intense new peak was observed at 1650 cm^{-1} (Figure 2D), which is due to the new carbonyl (C═O) stretching of amide I absorption

https://dx.doi.org/10.1021/acsabm.9b01111
ACS Appl. Bio Mater. 2020, 3, 1216−1225

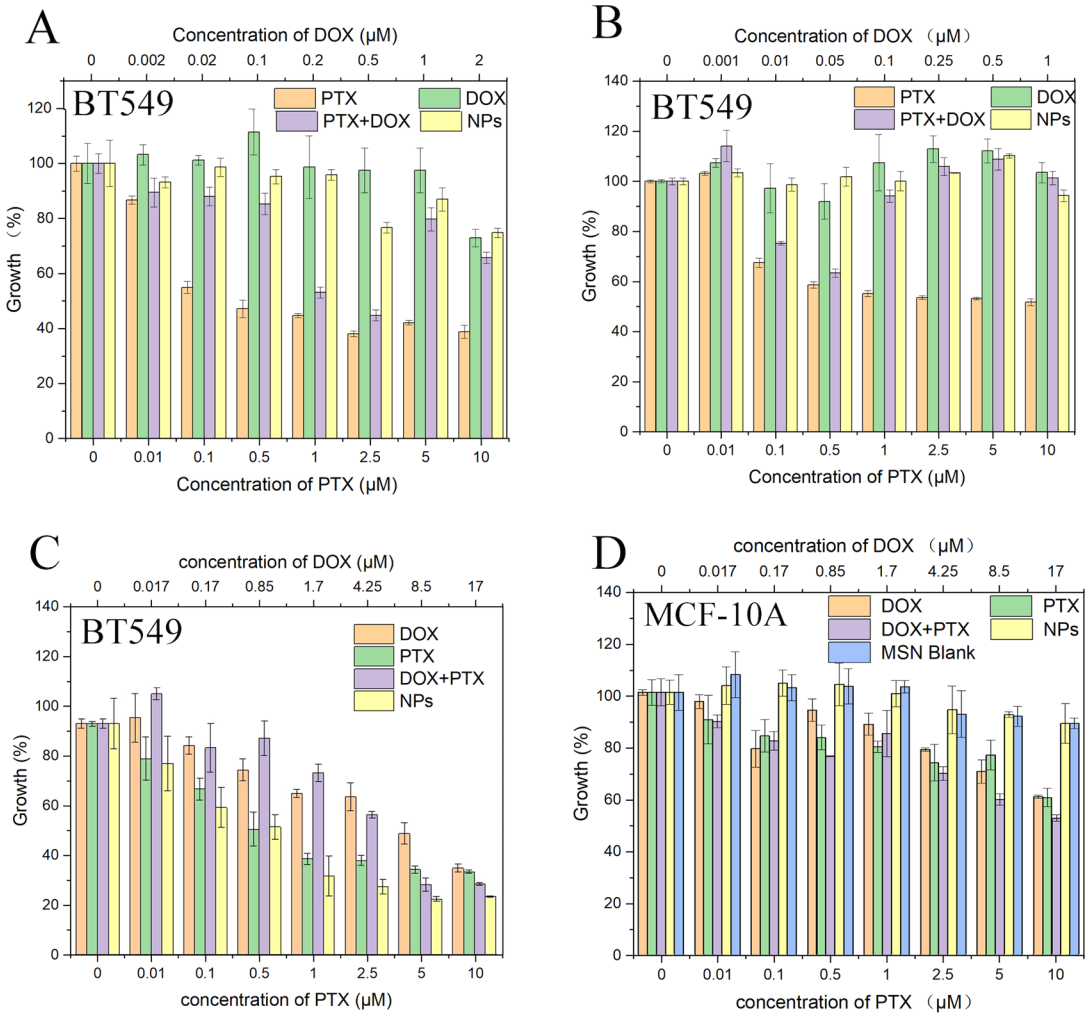

Figure 4. Cytotoxicity of PTX, DOX, DOX + PTX mixture, and drug loaded NPs for BT549 and MCF-10A and Blank MSN for MCF-10A. The molar ratios of DOX and PTX for BT549 cells are (A) 1:5, (B) 1:10, (C) 1:0.588; (D) The cytotoxicity of MCF-10A cells incubated with the ratio of DOX and PTX at 1:0.588. The blank MSN concentration corresponds to the content of the MSN in the drug loaded NPs. (n = 6).

(the most intense band centered at 1600−1700 cm^{-1}).[46] In addition, the binding rate of PTX is extremely high at around 94% (SI Table S1), almost all of the input drugs are covalently combined with MSN. With this advantage, we can precisely control the dosage of PTX to achieve the optimal drug loading ratio.[47]

Subsequently, a PSS layer was introduced by microfluidic technology (SI Figure S3). The water-soluble polymer PSS and MSN were added in the inner phase, and the ethanol served as the outer phase, when the two liquid meet together, PSS was nanosediment to the MSN surface. With decreasing pH value, more and more unmodified amino groups on MSN are protonated, and the electrostatic attraction will be destroyed. PSS membranes will change to a swelling and porous structure, which results in the rapid drug release.[36,48] As shown in TEM, a significant PSS shell layer was observed in the DOX@MSN-PTX@PSS NPs (Figure 2A). the DLS results showed the zeta potential of DOX@MSN-PTX was adjusted to around 3 mV by PSS which can significantly reduce the nonspecific phagocytosis by healthy cells (Figure 2C).[37] Overall, according to the results, we have successfully synthesized DOX@MSN-PTX@PSS NPs.

3.3. In Vitro DOX and PTX Release from the DOX@MSN-PTX@PSS NPs. The in vitro release profiles of the NPs at pH 5 or 7, in the absence or presence of DTT are shown in Figure 3. The results indicated that less than 13% of PTX released at pH 7 without DTT after 20 h. The cumulative PTX release was stimulated by DTT and increased to 30% at 20 h. Acidic pH 5 also had minor stimulation effect on PTX release, whereas the PTX release had been greatly stimulated in the presence of DTT plus pH 5, which reached to around 35% at 20 h. The release profile of DOX showed a similar trend compared to PTX, both the pH 5 and DTT had stimulated DOX release, and the cumulative DOX release increased significantly to around 70% at 20 h at pH 5 with DTT (Figure 3B). The drug release from DOX@MSN-PTX@PSS depends on two factors, the PSS layer with acidic pH responsive and the PTX layer with redox responsive. Under acidic conditions, unmodified amino groups of MSN-NH_2 are protonated and the electrostatic attraction with PSS declined. PSS membranes changed to a swelling and porous structure; moreover, the protonated DOX also has a reduced force with PSS, and therefore resulted in the rapid DOX release.[36,48] The release of PTX layer depends on the redox condition, therefore DTT stimulated both PTX and DOX release. Moreover, under two simulated conditions, the DOX and PTX release has significantly increased, which reflects that double response

https://dx.doi.org/10.1021/acsabm.9b01111
ACS Appl. Bio Mater. 2020, 3, 1216−1225

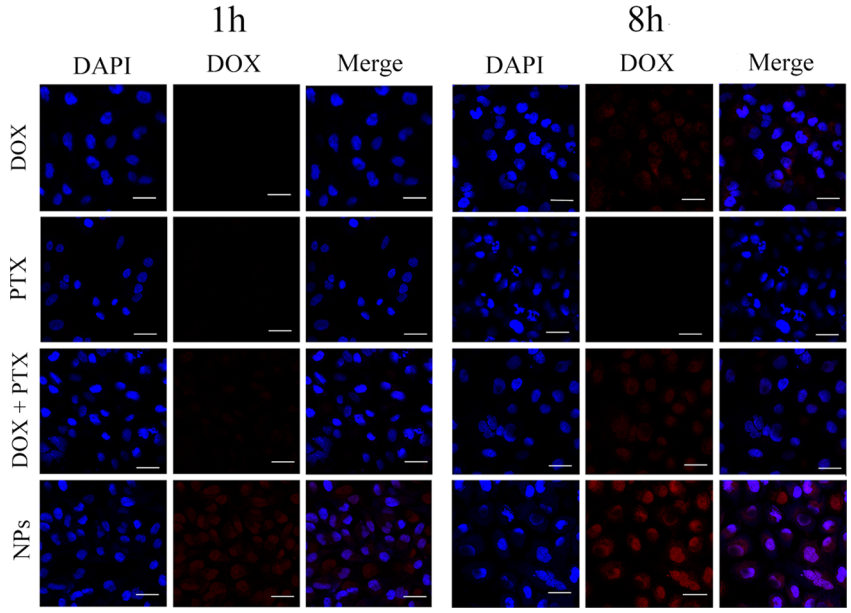

Figure 5. Confocal microscopy images of DOX, PTX, DOX + PTX and drug loaded NPś uptake in BT549 cells. The scale bars denote 20 μm.

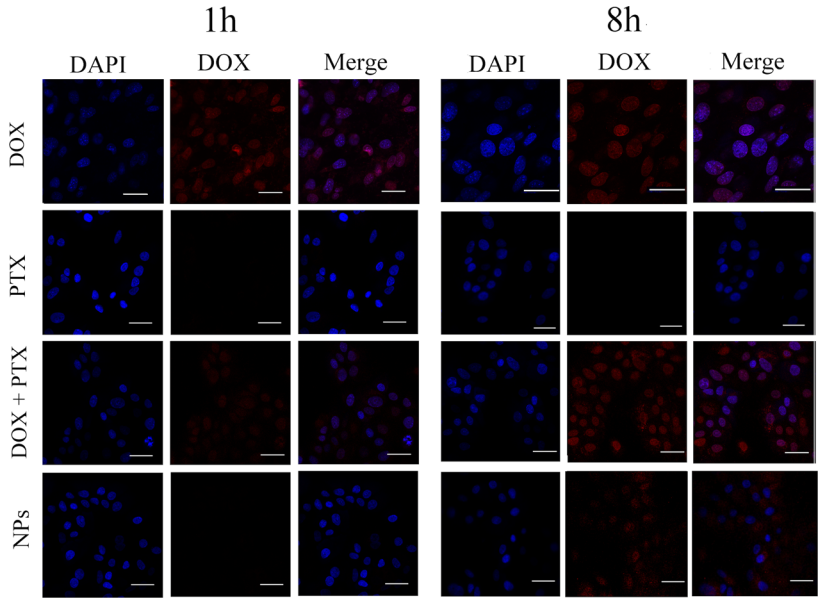

Figure 6. Confocal microscopy images of cellular uptake of DOX, PTX, DOX + PTX, and NPs of MCF-10A. Scale bars denote 20 μm.

nanoparticles are more precise in controlling drug release than the single response nanoparticles.

3.4. In Vitro Cytotoxicity and Cell Apoptosis. The cell viabilities of DOX, PTX, DOX + PTX, and NPs were studied by using WST-1 assay for breast cancer cell BT549 and healthy breast cell MCF-10A. The drug loading ratio of PTX and DOX can be controlled by adjusting the drug loading time and DOX concentration in loading buffer and the input content of PTX-SS-COOH in the reaction. Particles with different molar ratios of DOX: PTX were prepared. As shown in Figure 4A and B, when the molar ratio of DOX and PTX was 1:5 or 1:10, DOX +PTX mixture and NPs showed no inhibition effect toward BT549 cells compared to pure DOX and PTX, which indicated that high concentrations of PTX cannot induce cell apoptosis compared with low concentrations.[47,49,50] This may because PTX activates the extracellular signal-regulated kinase,[51] leading to cell proliferation and inducing the drug resistance.[52] Therefore, it was important to control the PTX loading ratio to DOX in MSN in order to obtain optimal synergistic effect. Figure 4C demonstrates that both PTX-DOX mixture and drug loaded NPs induced significant cell viability on BT549 cells at a DOX to PTX molar ratio 1:0.588 in a synergistic manner. This novel nanoparticle that can precisely control the delivery ratio of DOX and PTX is highly demanded for PTX/DOX delivery. In terms of healthy cells, both pure MSN and the drug loaded NPs do not alter the cell viability (Figure 4D), which proves that the novel drug loaded NPs are highly selective for inhibiting the cancer cells.

3.5. Cellular Uptake. To verify the DOX uptake in cancer cell and in healthy cell, free DOX, PTX, PTX+DOX, and drug loaded NPs were incubated with BT549 and MCF-10A cells for 1 or 8 h. DAPI was used for nuclear staining, and the DOX

https://dx.doi.org/10.1021/acsabm.9b01111
ACS Appl. Bio Mater. 2020, 3, 1216−1225

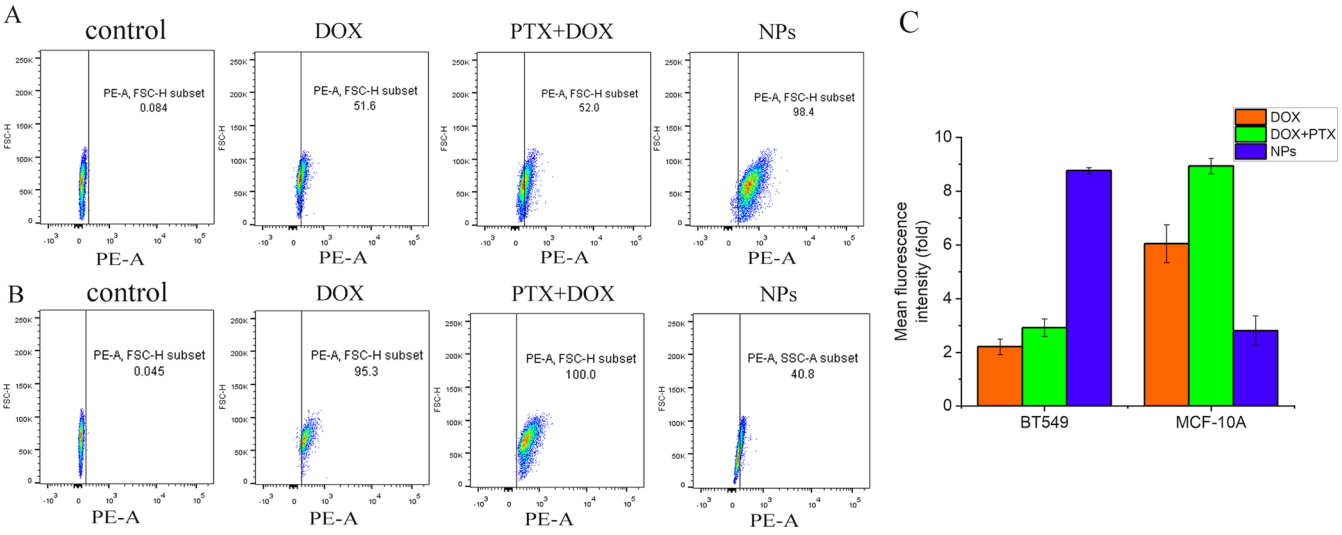

Figure 7. Flow cytometry of cellular uptake of DOX, PTX, DOX + PTX, and NPs. (A) flow cytometry of uptake in BT549, (B) MCF-10A cells, and (C) Mean fluorescence intensity of drug.

fluorescence was monitored in cells by CLSM. The NPs with DOX/PTX loading ratio of 1:0.588 was selected for this experiment.

As shown in Figure 5, a sporadic red fluorescence signal was observed in the free DOX and PTX+DOX group because pure DOX can also be internalized into the cell. In contrast, nearly 4 times the fluorescence intensity was observed inside the nuclei for the NPś group as indicated in the flow cytometry results (Figure 7A,C). These results strongly confirm that NPs with optimum DOX/PTX ratio were apparently ingested by cancer cell BT-549. Since NPs encounter the acidic and redox microenvironment in tumor cells, the PSS layer became porous and the double-sulfur linker broke, thus prompting the rapid release of PTX and DOX. The DOX colocalization at the nucleus can prove that the drug is released from the NPs (Figure 5). More importantly, PSS is an ionic polyelectrolyte polymer, when the NPś neutral zeta-potential is disrupted and became positive, PSS can be altered to an uptake enhancing factor, which not only increases lipophilicity but also facilitates the entry of NPs into cancer cells via caveolae-mediated endocytosis.[53,54] Therefore, these results strongly confirmed that the NPś uptake was improved in cancer cells.[55,56]

Meanwhile, Figure 6 shows that in the NPs group, the DOX fluorescence intensity is only half or one-third of the fluorescence intensity comparing with the free DOX and PTX+DOX group from healthy cells MCF-10A (Figure 7B,C), indicating that fewer NPs have been uptaken by MCF-10A after incubating for 8 h. Since there's no acidic or redox environment in the healthy MCF-10A cells, the PSS layer and disulfide bond are stable, and the neutral zeta potential in NPs can prevent them from uptaking into MCF-10A cells. These results indicate the NPs did not degrade under a healthy cell environment, and the DOX cannot be released from the NPs into the healthy cells and nuclear.

Overall, the NPs have the specific DOX releasing ability which can reduce the damage to the healthy cells. Therefore, it is a promising system for eliminating possible side effects compared with pure drugs.

4. CONCLUSION

In this work, we have prepared an MSN-based pH and redox dual responsive drug delivery system for DOX and PTX codelivery with precise control of the drug ratio. DOX was directly loaded in the pores of MSN, whereas PTX was conjugated to MSN through three steps of chemical reactions, via a linker with a disulfide bond, thus could control the DOX and PTX release by redox responsive. This rational design not only can increase the stability, dispersibility, and loading degree of the hydrophobic drug PTX, but it also enables the flexible adjustment of drug loading ratio to DOX, which is important for generating the best synergistical effect. In addition, the surface-coated PSS provided the system with acidic responsive, and more importantly, adjust the surface charge to be approximately neutral, which is beneficial to reduce nonspecific endocytosis by healthy cells. We found that the two indispensable release conditions of acidity and reduction must be met simultaneously, then the drug can be rapidly and sufficiently released from the NPs, which can greatly increase the tumor specificity of the drug. Moreover, the cell experiments showed that NPs could effectively and selectively kill cancer cells BT549 but had no inhibition effect on healthy cells MCF-10A. Confocal and flow cytometry results also confirmed that NPs could be endocytosed by BT549 and release the DOX, which accumulated into the nucleus within 1h. Nevertheless, for healthy cells, after 8 h of culturing, endocytosis of NPs was neglectable, and very limited DOX was released from the MSN and accumulated in the nucleus. Overall, the nanoplatform has significantly specialized on cancer cells to reduce the adverse drug effect and can precisely load DOX and PTX at optimum ratio to generate the best synergistical effect, thus it is a promising nanoplatform for future clinical delivery of DOX/PTX combination.

■ ASSOCIATED CONTENT

Supporting Information

The Supporting Information is available free of charge at https://pubs.acs.org/doi/10.1021/acsabm.9b01111.

Figures S1−S3 and Table S1. Experimental details, instrument parameters, and operating procedures (PDF)

https://dx.doi.org/10.1021/acsabm.9b01111
ACS Appl. Bio Mater. 2020, 3, 1216−1225

AUTHOR INFORMATION

Corresponding Authors

Fan Yang − *The Center for Drug Research and Development and Engineering & Technology Research Center for Topical Precise Drug Delivery System, School of Pharmacy, Guangdong Pharmaceutical University, Guangzhou 510006, China*; Email: gzyangfan@hotmail.com

Hongbo Zhang − *Pharmaceutical Sciences Laboratory and Turku Bioscience Center, Åbo Akademi University, FI-20520 Turku, Finland; Department of Radiology, Affiliated Hospital of Jiangsu University, Jiangsu University, 212001 Zhenjiang, P.R. China*; orcid.org/0000-0002-1071-4416; Email: hongbo.zhang@abo.fi

Authors

Jiaqi Yan − *The Center for Drug Research and Development and Engineering & Technology Research Center for Topical Precise Drug Delivery System, School of Pharmacy, Guangdong Pharmaceutical University, Guangzhou 510006, China; Pharmaceutical Sciences Laboratory and Turku Bioscience Center, Åbo Akademi University, FI-20520 Turku, Finland*

Xiaoyu Xu − *Pharmaceutical Sciences Laboratory and Turku Bioscience Center, Åbo Akademi University, FI-20520 Turku, Finland*

Junnian Zhou − *Pharmaceutical Sciences Laboratory and Turku Bioscience Center, Åbo Akademi University, FI-20520 Turku, Finland; Experimental Hematology and Biochemistry Lab, Beijing Institute of Radiation Medicine, Beijing 100850, China*

Chang Liu − *Pharmaceutical Sciences Laboratory and Turku Bioscience Center, Åbo Akademi University, FI-20520 Turku, Finland*

Lirong Zhang − *Department of Radiology, Affiliated Hospital of Jiangsu University, Jiangsu University, 212001 Zhenjiang, P.R. China*

Dongqing Wang − *Department of Radiology, Affiliated Hospital of Jiangsu University, Jiangsu University, 212001 Zhenjiang, P.R. China*

Complete contact information is available at: https://pubs.acs.org/10.1021/acsabm.9b01111

Author Contributions

Each author contributed to the manuscript, and each author has approved the final version of the manuscript.

Author Contributions

⊥These authors contributed equally.

Notes

The authors declare no competing financial interest.

ACKNOWLEDGMENTS

This work was supported by Distinguished Clinical Investigator Grant of Jiangsu Province, China (Grant No. JSTP201701), Jiangsu Provincial Key Research and Development Programme (Grant No. BE2018690) and Sigrid Jusélius Foundation (decision no. 28001830K1). Prof. F. Yang acknowledges grants from the Technological Project of Guangzhou technology bureau (Grant number: 20170402199).

REFERENCES

(1) Li, N.; Sun, Q.; Yu, Z.; Gao, X.; Pan, W.; Wan, X.; Tang, B. Nuclear-Targeted Photothermal Therapy Prevents Cancer Recurrence with Near-Infrared Triggered Copper Sulfide Nanoparticles. *ACS Nano* **2018**, *12*, 5197−5206.

(2) Zhang, H.; Liu, D.; Wang, L.; Liu, Z.; Wu, R.; Janoniene, A.; Ma, M.; Pan, G.; Baranauskiene, L.; Zhang, L.; Cui, W.; Petrikaite, V.; Matulis, D.; Zhao, H.; Pan, J.; Santos, H. A. Microfluidic Encapsulation of Prickly Zinc-Doped Copper Oxide Nanoparticles with VD1142 Modified Spermine Acetalated Dextran for Efficient Cancer Therapy. *Adv. Healthcare Mater.* **2017**, *6* (11), 1601406.

(3) Zhang, Q.; Gong, Y.; Guo, X. J.; Zhang, P.; Ding, C. F. Multifunctional Gold Nanoparticle-Based Fluorescence Resonance Energy-Transfer Probe for Target Drug Delivery and Cell Fluorescence Imaging. *ACS Appl. Mater. Interfaces* **2018**, *10*, 34840−34848.

(4) Hu, D.; Chen, L.; Qu, Y.; Peng, J.; Chu, B.; Shi, K.; Hao, Y.; Zhong, L.; Wang, M.; Qian, Z. Oxygen-generating Hybrid Polymeric Nanoparticles with Encapsulated Doxorubicin and Chlorin e6 for Trimodal Imaging-Guided Combined Chemo-Photodynamic Therapy. *Theranostics* **2018**, *8* (6), 1558−1574.

(5) Zhao, D.; Zhang, H.; Yang, S.; He, W.; Luan, Y. Redox-sensitive mPEG-SS-PTX/TPGS mixed micelles: An efficient drug delivery system for overcoming multidrug resistance. *Int. J. Pharm.* **2016**, *515* (1−2), 281−292.

(6) Wu, J.; Tang, C.; Yin, C. Co-delivery of doxorubicin and interleukin-2 via chitosan based nanoparticles for enhanced antitumor efficacy. *Acta Biomater.* **2017**, *47*, 81−90.

(7) Sun, D.; Ding, J.; Xiao, C.; Chen, J.; Zhuang, X.; Chen, X. Preclinical evaluation of antitumor activity of acid-sensitive PEGylated doxorubicin. *ACS Appl. Mater. Interfaces* **2014**, *6* (23), 21202−14.

(8) Ma, Y.; Fan, X.; Li, L. pH-sensitive polymeric micelles formed by doxorubicin conjugated prodrugs for co-delivery of doxorubicin and paclitaxel. *Carbohydr. Polym.* **2016**, *137*, 19−29.

(9) Liang, Z.; Yang, Z.; Yuan, H.; Wang, C.; Qi, J.; Liu, K.; Cao, R.; Zheng, H. A protein@metal-organic framework nanocomposite for pH-triggered anticancer drug delivery. *Dalton Trans* **2018**, *47* (30), 10223−10228.

(10) Das, M.; Jain, R.; Agrawal, A. K.; Thanki, K.; Jain, S. Macromolecular bipill of gemcitabine and methotrexate facilitates tumor-specific dual drug therapy with higher benefit-to-risk ratio. *Bioconjugate Chem.* **2014**, *25* (3), 501−9.

(11) Caron, J.; Maksimenko, A.; Mougin, J.; Couvreur, P.; Desmaële, D. Combined antitumoral therapy with nanoassemblies of bolaform polyisoprenoyl paclitaxel/gemcitabine prodrugs. *Polym. Chem.* **2014**, *5* (5), 1662−1673.

(12) Arroyo-Crespo, J. J.; Deladriere, C.; Nebot, V. J.; Charbonnier, D.; Masiá, E.; Paul, A.; James, C.; Armiñán, A.; Vicent, M. J. Anticancer Activity Driven by Drug Linker Modification in a Polyglutamic Acid-Based Combination-Drug Conjugate. *Adv. Funct. Mater.* **2018**, *28* (22), 1800931.

(13) Chen, C.; Yao, W.; Sun, W.; Guo, T.; Lv, H.; Wang, X.; Ying, H.; Wang, Y.; Wang, P. A self-targeting and controllable drug delivery system constituting mesoporous silica nanoparticles fabricated with a multi-stimuli responsive chitosan-based thin film layer. *Int. J. Biol. Macromol.* **2019**, *122*, 1090−1099.

(14) Zeng, X.; Liu, G.; Tao, W.; Ma, Y.; Zhang, X.; He, F.; Pan, J.; Mei, L.; Pan, G. A Drug-Self-Gated Mesoporous Antitumor Nanoplatform Based on pH-Sensitive Dynamic Covalent Bond. *Adv. Funct. Mater.* **2017**, *27* (11), 1605985.

(15) Yan, Q.; Guo, X.; Huang, X.; Meng, X.; Liu, F.; Dai, P.; Wang, Z.; Zhao, Y. Gated Mesoporous Silica Nanocarriers for Hypoxia-Responsive Cargo Release. *ACS Appl. Mater. Interfaces* **2019**, *11* (27), 24377−24385.

(16) Llopis-Lorente, A.; Garcia-Fernandez, A.; Murillo-Cremaes, N.; Hortelao, A. C.; Patino, T.; Villalonga, R.; Sancenon, F.; Martinez-Manez, R.; Sanchez, S. Enzyme-Powered Gated Mesoporous Silica Nanomotors for On-Command Intracellular Payload Delivery. *ACS Nano* **2019**, *13* (10), 12171−12183.

(17) Chen, T.-H.; Zhang, S.; Jaishi, M.; Adhikari, R.; Bi, J.; Fang, M.; Xia, S.; Zhang, Y.; Luck, R. L.; Pati, R.; Hsien-Ming, L.; Luo, F.-T.; Tiwari, A.; Liu, H. New Near-Infrared Fluorescent Probes with Single-

Photon Anti-Stokes-Shift Fluorescence for Sensitive Determination of pH Variances in Lysosomes with a Double-Checked Capability. *ACS Applied Bio Materials* **2018**, *1* (3), 549−560.
(18) Xie, W.; Deng, W. W.; Zan, M.; Rao, L.; Yu, G. T.; Zhu, D. M.; Wu, W. T.; Chen, B.; Ji, L. W.; Chen, L.; Liu, K.; Guo, S. S.; Huang, H. M.; Zhang, W. F.; Zhao, X.; Yuan, Y.; Dong, W.; Sun, Z. J.; Liu, W. Cancer Cell Membrane Camouflaged Nanoparticles to Realize Starvation Therapy Together with Checkpoint Blockades for Enhancing Cancer Therapy. *ACS Nano* **2019**, *13* (3), 2849−2857.
(19) Yao, M.; Ma, M.; Zhang, H.; Zhang, Y.; Wan, G.; Shen, J.; Chen, H.; Wu, R. Mesopore-Induced Aggregation of Cobalt Protoporphyrin for Photoacoustic Imaging and Antioxidant Protection of Stem Cells. *Adv. Funct. Mater.* **2018**, *28* (47), 1804497.
(20) Yang, B.; Chen, Y.; Shi, J. Exogenous/Endogenous-Triggered Mesoporous Silica Cancer Nanomedicine. *Adv. Healthcare Mater.* **2018**, *7* (20), No. e1800268.
(21) Tang, Y.; Hu, H.; Zhang, M. G.; Song, J.; Nie, L.; Wang, S.; Niu, G.; Huang, P.; Lu, G.; Chen, X. An aptamer-targeting photoresponsive drug delivery system using "off-on" graphene oxide wrapped mesoporous silica nanoparticles. *Nanoscale* **2015**, *7* (14), 6304−10.
(22) Llinas, M. C.; Martinez-Edo, G.; Cascante, A.; Porcar, I.; Borros, S.; Sanchez-Garcia, D. Preparation of a mesoporous silica-based nano-vehicle for dual DOX/CPT pH-triggered delivery. *Drug Delivery* **2018**, *25* (1), 1137−1146.
(23) Liu, J.; Liang, H.; Li, M.; Luo, Z.; Zhang, J.; Guo, X.; Cai, K. Tumor acidity activating multifunctional nanoplatform for NIR-mediated multiple enhanced photodynamic and photothermal tumor therapy. *Biomaterials* **2018**, *157*, 107−124.
(24) Li, X.; Wu, M.; Pan, L.; Shi, J. Tumor vascular-targeted co-delivery of anti-angiogenesis and chemotherapeutic agents by mesoporous silica nanoparticle-based drug delivery system for synergetic therapy of tumor. *Int. J. Nanomed.* **2015**, *11*, 93−105.
(25) Jiamei, L.; Anchao, F.; Jinying, Y. J. P. I. C., Synthesis and Controllable Drug Release of Stimuli-Responsive Star Polymer. *2015*, *27* (5), 522−531.
(26) Huang, Q.; Bao, C.; Lin, Y.; Chen, J.; Liu, Z.; Zhu, L. Disulfide-phenylazide: a reductively cleavable photoreactive linker for facile modification of nanoparticle surfaces. *J. Mater. Chem. B* **2013**, *1* (8), 1125−1132.
(27) Liu, D.; Chen, Y.; Feng, X.; Deng, M.; Xie, G.; Wang, J.; Zhang, L.; Liu, Q.; Yuan, P. Micellar nanoparticles loaded with gemcitabine and doxorubicin showed synergistic effect. *Colloids Surf., B* **2014**, *113*, 158−68.
(28) Kawaguchi, K.; Higuchi, T.; Li, S.; Han, Q.; Tan, Y.; Igarashi, K.; Zhao, M.; Miyake, K.; Kiyuna, T.; Miyake, M. J. B.; communications, b. r., Combination therapy of tumor-targeting Salmonella typhimurium A1-R and oral recombinant methioninase regresses a BRAF-V600E-negative melanoma. **2018**, *503* (4), 3086−3092.
(29) Felgueiras, H.; Migonney, V. Sulfonate groups grafted on Ti6Al4V favor MC3T3-E1 cell performance in serum free medium conditions. *Mater. Sci. Eng., C* **2014**, *39*, 196−202.
(30) Zhang, H.; Liu, D.; Shahbazi, M. A.; Makila, E.; Herranz-Blanco, B.; Salonen, J.; Hirvonen, J.; Santos, H. A. Fabrication of a multifunctional nano-in-micro drug delivery platform by microfluidic templated encapsulation of porous silicon in polymer matrix. *Adv. Mater.* **2014**, *26* (26), 4497−503.
(31) Liu, D.; Zhang, H.; Fontana, F.; Hirvonen, J. T.; Santos, H. A. Microfluidic-assisted fabrication of carriers for controlled drug delivery. *Lab Chip* **2017**, *17* (11), 1856−1883.
(32) Herranz-Blanco, B.; Ginestar, E.; Zhang, H.; Hirvonen, J.; Santos, H. A. Microfluidics platform for glass capillaries and its application in droplet and nanoparticle fabrication. *Int. J. Pharm.* **2017**, *516* (1−2), 100−105.
(33) Zhang, H.; Cui, W.; Qu, X.; Wu, H.; Qu, L.; Zhang, X.; Makila, E.; Salonen, J.; Zhu, Y.; Yang, Z.; Chen, D.; Santos, H. A.; Hai, M.; Weitz, D. A. Photothermal-responsive nanosized hybrid polymersome as versatile therapeutics codelivery nanovehicle for effective tumor suppression. *Proc. Natl. Acad. Sci. U. S. A.* **2019**, *116* (16), 7744−7749.
(34) Ahn, J.; Ko, J.; Lee, S.; Yu, J.; Kim, Y.; Jeon, N. L. Microfluidics in nanoparticle drug delivery; From synthesis to pre-clinical screening. *Adv. Drug Delivery Rev.* **2018**, *128*, 29−53.
(35) Kim, Y.; Langer, Y. K. R. Microfluidics in Nanomedicine. *Rev. Cell Biol. Mol. Med.* **2015**, *1*, 127−152.
(36) Venkatesan, R.; Pichaimani, A.; Hari, K.; Balasubramanian, P. K.; Kulandaivel, J.; Premkumar, K. Doxorubicin conjugated gold nanorods: a sustained drug delivery carrier for improved anticancer therapy. *J. Mater. Chem. B* **2013**, *1* (7), 1010−1018.
(37) Honary, S.; Zahir, F. Effect of Zeta Potential on the Properties of Nano-Drug Delivery Systems - A Review (Part 2). *Trop. J. Pharm. Res.* **2013**, *12* (2), 1596−9827.
(38) Zheng, X.; Li, Z.; Chen, L.; Xie, Z.; Jing, X. Self-Assembly of Porphyrin−Paclitaxel Conjugates Into Nanomedicines: Enhanced Cytotoxicity due to Endosomal Escape. *Chem. - Asian J.* **2016**, *11* (12), 1780−1784.
(39) Yin, T.; Wu, Q.; Wang, L.; Yin, L.; Zhou, J.; Huo, M. Well-defined redox-sensitive polyethene glycol−paclitaxel prodrug conjugate for tumor-specific delivery of paclitaxel using octreotide for tumor targeting. *Mol. Pharmaceutics* **2015**, *12* (8), 3020−3031.
(40) Ma, X.; Ozliseli, E.; Zhang, Y.; Pan, G.; Wang, D.; Zhang, H. Fabrication of redox-responsive doxorubicin and paclitaxel prodrug nanoparticles with microfluidics for selective cancer therapy. *Biomater. Sci.* **2019**, *7* (2), 634−644.
(41) Shen, D.; Yang, J.; Li, X.; Zhou, L.; Zhang, R.; Li, W.; Chen, L.; Wang, R.; Zhang, F.; Zhao, D. Biphase stratification approach to three-dimensional dendritic biodegradable mesoporous silica nanospheres. *Nano Lett.* **2014**, *14* (2), 923−32.
(42) Liu, D.; Cito, S.; Zhang, Y.; Wang, C. F.; Sikanen, T. M.; Santos, H. A. A versatile and robust microfluidic platform toward high throughput synthesis of homogeneous nanoparticles with tunable properties. *Adv. Mater.* **2015**, *27* (14), 2298−2304.
(43) Herranz-Blanco, B.; Ginestar, E.; Zhang, H.; Hirvonen, J.; Santos, H. A. Microfluidics platform for glass capillaries and its application in droplet and nanoparticle fabrication. *Int. J. Pharm.* **2017**, *516* (1−2), 100−105.
(44) Huo, Q.; Zhu, J.; Niu, Y.; Shi, H.; Gong, Y.; Li, Y.; Song, H.; Liu, Y. pH-triggered surface charge-switchable polymer micelles for the co-delivery of paclitaxel/disulfiram and overcoming multidrug resistance in cancer. *Int. J. Nanomed.* **2017**, *12*, 8631−8647.
(45) Maguire, C. M.; Rösslein, M.; Wick, P.; Prina-Mello, A. Characterisation of particles in solution − a perspective on light scattering and comparative technologies. *Sci. Technol. Adv. Mater.* **2018**, *19* (1), 732−745.
(46) Mallamace, F.; Corsaro, C.; Mallamace, D.; Vasi, S.; Vasi, C.; Dugo, G. The role of water in protein's behavior: The two dynamical crossovers studied by NMR and FTIR techniques. *Comput. Struct. Biotechnol. J.* **2015**, *13*, 33−7.
(47) Markovsky, E.; Baabur-Cohen, H.; Satchi-Fainaro, R. Anticancer polymeric nanomedicine bearing synergistic drug combination is superior to a mixture of individually-conjugated drugs. *J. Controlled Release* **2014**, *187*, 145−57.
(48) Zhao, J.; Li, X.; Wang, X.; Wang, X. Fabrication of Hybrid Nanostructures Based on Fe3O4 Nanoclusters as Theranostic Agents for Magnetic Resonance Imaging and Drug Delivery. *Nanoscale Res. Lett.* **2019**, *14* (1), 200.
(49) Wang, Y.; Zhang, H.; Hao, J.; Li, B.; Li, M.; Xiuwen, W. Lung cancer combination therapy: co-delivery of paclitaxel and doxorubicin by nanostructured lipid carriers for synergistic effect. *Drug Delivery* **2016**, *23* (4), 1398−403.
(50) Feng, T.; Tian, H.; Xu, C.; Lin, L.; Xie, Z.; Lam, M. H.; Liang, H.; Chen, X. Synergistic co-delivery of doxorubicin and paclitaxel by porous PLGA microspheres for pulmonary inhalation treatment. *Eur. J. Pharm. Biopharm.* **2014**, *88* (3), 1086−93.
(51) Baati, T.; Njim, L.; Neffati, F.; Kerkeni, A.; Bouttemi, M.; Gref, R.; Najjar, M. F.; Zakhama, A.; Couvreur, P.; Serre, C.; Horcajada, P. In depth analysis of the in vivo toxicity of nanoparticles of porous

https://dx.doi.org/10.1021/acsabm.9b01111
ACS Appl. Bio Mater. 2020, 3, 1216−1225

iron(iii) metal−organic frameworks. *Chemical Science* **2013**, *4* (4), 1597−1607.
(52) Liu, Y.; Fang, J.; Kim, Y. J.; Wong, M. K.; Wang, P. Codelivery of doxorubicin and paclitaxel by cross-linked multilamellar liposome enables synergistic antitumor activity. *Mol. Pharmaceutics* **2014**, *11* (5), 1651−61.
(53) Voigt, J.; Christensen, J.; Shastri, V. P. Differential uptake of nanoparticles by endothelial cells through polyelectrolytes with affinity for caveolae. *Proc. Natl. Acad. Sci. U. S. A.* **2014**, *111* (8), 2942−7.
(54) Quang, H. V.; Chang, C. C.; Song, P.; Hauge, E. M.; Kjems, J. Caveolae-mediated mesenchymal stem cell labelling by PSS-coated PLGA PFOB nano-contrast agent for MRI. *Theranostics* **2018**, *8* (10), 2657−2671.
(55) Kunwar, A.; Barik, A.; Mishra, B.; Rathinasamy, K.; Pandey, R.; Priyadarsini, K. I. Quantitative cellular uptake, localization and cytotoxicity of curcumin in normal and tumor cells. *Biochim. Biophys. Acta, Gen. Subj.* **2008**, *1780* (4), 673−9.
(56) Gao, C.; Tang, F.; Gong, G.; Zhang, J.; Hoi, M. P. M.; Lee, S. M. Y.; Wang, R. pH-Responsive prodrug nanoparticles based on a sodium alginate derivative for selective co-release of doxorubicin and curcumin into tumor cells. *Nanoscale* **2017**, *9* (34), 12533−12542.

https://dx.doi.org/10.1021/acsabm.9b01111
ACS Appl. Bio Mater. 2020, 3, 1216−1225